Rea, D.K., Basov, I.A., Scholl, D.W., and Allan, J.F. (Eds.), 1995
Proceedings of the Ocean Drilling Program, Scientific Results, Vol. 145

28. IDENTIFICATION AND CHARACTERIZATION OF THE CRETACEOUS/TERTIARY BOUNDARY AT ODP SITES 886 AND 803 AND DSDP SITE 576[1]

Frank T. Kyte,[2] Jennifer A. Bostwick,[2] and Lei Zhou[2]

ABSTRACT

The Cretaceous/Tertiary (K/T) boundary Ir anomaly has been identified in deep-sea clays at three new localities in the North Pacific: Ocean Drilling Program Site 886 near the Chinook Trough (44°41.4′N, 168°14.4′W), ODP Site 803 on the Ontong-Java Plateau (2°26.0′N, 160°32.5′E), and Deep Sea Drilling Project Site 576 in the western North Pacific (32°21.4′N, 164°16.5′E). At each of these sites, the K/T boundary is characterized by a large Ir anomaly, coincident with minor enrichments of Cr and abundant shocked quartz and magnesioferrite spinel. Spheroidal material has also been observed in K/T boundary sediments at ODP Site 886 and DSDP Site 576. The magnitude of the Ir anomaly is comparable to that observed at other marine sites around the world, with estimated net fluences of 52, 140, 130, and 90 ng Ir cm^{-2} in Holes 886C, 803D, 576, and 576B, respectively. At Sites 803 and 576, some biostratigraphic control was available from poorly preserved nannofossils and ichthyoliths, respectively. At Site 886, it was necessary to survey Ir concentrations across a 18.1- meter-thick unit of clay (54.3 to 72.4 mbsf) known to record sedimentation from 80 to 10 Ma.

INTRODUCTION

The Cretaceous/Tertiary (K/T) boundary is one of the most important and distinctive stratigraphic horizons in the marine sedimentary record. It marks one of the greatest mass extinctions in Earth history (e.g., Sepkoski, 1982). At localities where it is well preserved, the boundary is characterized by anomalous concentrations of Ir (Alvarez et al., 1980) and other siderophile elements (Smit and Hertogen, 1980; Ganapathy, 1980; Kyte et al., 1980). At many K/T boundary localities, the geochemical anomaly is coincident with abundant shocked minerals (Bohor et al., 1987) and spheroidal debris (Smit and Klaver, 1981; Montanari et al., 1983). High-temperature mineral phases have been identified in some spherules (e.g., Smit and Kyte, 1984; Kyte and Smit, 1986; Bohor et al., 1986). The siderophile element and mineralogical anomalies are commonly attributed to an asteroid or comet impact at the end of the Cretaceous Period, as was first hypothesized by Alvarez et al. (1980). The recent discovery of a candidate for the K/T impact site, the Chicxulub structure (Hildebrand et al., 1991; Sharpton et al., 1992) on the Yucatán Peninsula, has lent considerable credence to this hypothesis.

An understanding of the physical and biological processes that were important at the K/T transition relies on interpretation of an imperfect, and often sparse, geologic record. One portion of the record that is poorly represented is that of the ancestral Pacific. At 66 Ma the Pacific basin made up >30% of the Earth's surface; the region directly west of the Chicxulub impact structure and important K/T sections around the Gulf of Mexico and in the North American interior (e.g., Smit et al., 1992; Izett, 1990). The record of this once-vast region is now found only on the Mesozoic-age crust of the western Pacific Plate (Fig. 1).

Before this study, only four K/T boundary sections with intact geochemical and mineralogical anomalies had been reported on the Pacific Plate. These included two calcareous sequences on the Shatsky and Hess rises; DSDP Site 577 (Heath, Burckle, et al., 1985; Michel et al., 1985) and DSDP Site 465 (Thiede, Vallier, et al., 1981; Kyte et al., 1980). The other two K/T boundaries were found in pelagic clays in Core LL44-GPC3 (Kyte and Wasson, 1986) and at DSDP Site 596 (Zhou et al., 1991).

In this paper we report the identification of three new K/T boundaries on the Pacific Plate. One of these is in sediments from ODP Hole 886C, recently recovered from near the Chinook Trough in the North Pacific (Rea, Basov, Janecek, Palmer-Julson, et al., 1993). The other two are from previously drilled sites on the Ontong-Java Plateau (ODP Site 803; Kroenke, Berger, Janecek, et al., 1991) and in the western North Pacific (DSDP Site 576; Heath, Burckle, et al., 1985). The K/T boundary at these three sites are all in clays and their value to K/T research will be as a source of material for analysis of the geochemical and mineralogical anomalies associated with the K/T event. At ODP Site 886, identification of the K/T boundary also provides important stratigraphic constraints on sediments that otherwise lack any distinguishable stratigraphic datums older than the late Miocene.

SAMPLES AND PROCEDURES

Our basic methodology began with a search for an Ir anomaly in sediments of the appropriate age. If one was found, sediments were resampled to confirm the anomaly by replicate analysis, defined with more closely spaced samples, and trace mineral separates were investigated for evidence of high-pressure and high-temperature mineral phases diagnostic of the K/T boundary. Sample sizes for the initial survey were typically 0.5 to 1 cm^3, enough material for chemical analysis. Subsequent samples were typically ~2 cm^3, providing additional material for mineralogical analyses.

We sampled the entire length of ODP Hole 886C with 137 samples. Recovery at this hole consisted of 72.4 m of pelagic clays and diatomaceous oozes (Rea, Basov, Janecek, Palmer-Julson, et al., 1993). At the time of our initial sampling the oldest biostratigraphic datum available indicated that diatomaceous sediments at 54.3 mbsf were late Miocene in age. The underlying 18.1 m of clays were of undetermined age. We took one sample per section of core from the top to 48.55 mbsf (145-886C-6H-3, 75–76 cm; 32 samples). We sampled the rest of Core 145-886C-6H at ~50 cm intervals (10 samples to 54.05 mbsf). The other 95 samples were from Cores 145-886C-7H and -8H (Unit III of Rea, Basov, Janecek, Palmer-Julson, et al., 1993) at ~20-cm intervals. Subsequent sampling concentrated on intervals from 55.25 to 56.00 mbsf (10 samples) and from 64.95 to 65.55 mbsf (17 samples).

Samples from ODP Hole 803D were taken at ~10-cm intervals in Section 130-803D-68R-1 from 10 to 120 cm (621.9 to 623.0 mbsf).

[1] Rea, D.K., Basov, I.A., Scholl, D.W., and Allan, J.F. (Eds.), 1995. *Proc. ODP, Sci. Results,* 145: College Station, TX (Ocean Drilling Program).

[2] Institute of Geophysics and Planetary Physics, University of California, Los Angeles, CA 90024, U.S.A.

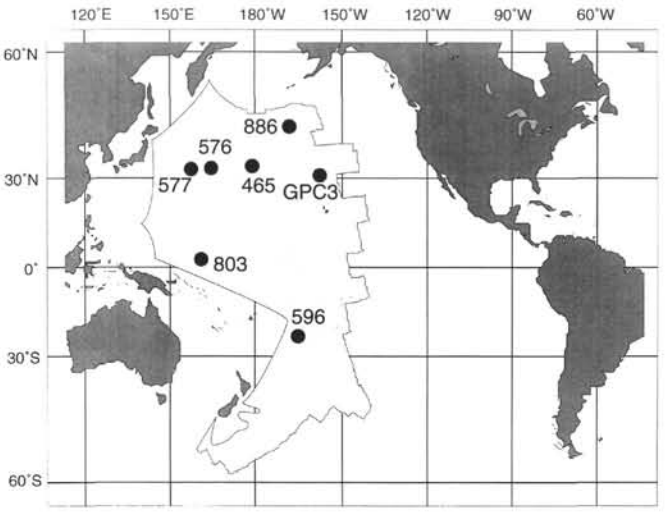

Figure 1. Map of Pacific deep-sea localities that have intact K/T boundaries, including three new sites described in this paper. Outline of the Mesozoic portion of the Pacific Plate is highlighted.

Initial reports on this hole indicated that the K/T boundary was thought to be at 622.25–622.29 mbsf based on poorly preserved nannofossil remains (Kroenke, Berger, Janecek, et al., 1991). Subsequent sampling was 8 samples at ~3- and 4-cm intervals from 622.31 to 622.55 mbsf.

Initial sampling of sediments from DSDP Site 576 was with a suite of 153 samples from three holes that sampled the upper 58.82 m of the composite section of Heath et al. (1985). Samples were splits of X-ray fluorescence pellets used for major element analyses by Heath et al. (1985). We concentrated on the interval from 52 to 56 mbsf which contained the K/T interval as defined by ichthyolith biostratigraphy (Doyle and Riedel, 1985). In this paper, we will report only results from analyses of sediments from the vicinity of the K/T boundary. Subsequent to our initial survey, we obtained and analyzed new samples from DSDP Holes 576 (16 samples; 86-576-8-1, 7 cm, to 86-576-8-1, 147 cm) and 576B (26 samples; 86-576B-6-3, 1 cm, to 86-576B-6-4, 138 cm).

Samples for chemical analyses are dried at 200°C (high temperatures are to degas potential organic matter before neutron irradiation) and then ground in a high-purity alumina mortar. Splits of ~80 to 100 mg are pressed into pellets with a tool-steel die and then individually wrapped in high-purity Al foil. Samples, control rock powders, and standard solutions (dried onto Al foil) are packaged together and irradiated for 5 hr at the University of Missouri research reactor facility at a neutron flux of $\sim 7 \times 10^{13}$ n cm^{-2} s^{-1}. Initially, samples are counted ~4–8 weeks following irradiation for ~24 hr, on intrinsic Ge coaxial gamma-ray detectors with resolutions ranging from 1.75 to 1.90 keV at 1.3 MeV. We look for characteristic ^{192}Ir gammas at 316.5 and 468.1 keV. Whole-rock detection limits for Ir by instrumental neutron activation analysis (INAA) are ~2–3 ng/g for pelagic clays. Detection limits are largely a function of the concentrations of Eu, Sc, and Co. Iridium concentrations in most samples are considerably below INAA detection limits and require chemical purification of Ir. Radiochemical procedures are those described by Kyte et al. (1993). Purified Ir samples are then counted for 12 to 48 hr. Detection limits for Ir by radiochemical neutron activation analysis (RNAA) are typically 0.02 to 0.05 ng/g for the conditions cited above, but can be higher in samples with low chemical yields.

Trace mineral separates are prepared from splits of selected samples that are thought to contain the K/T boundary. Clays are dried at 100°C, dispersed with a sodium hexametaphosphate solution and fine fractions are pipetted off. Biogenic and authigenic components were removed by acid (oxalic, HCl) digestion and residues were etched with HF. In typical K/T boundary sediments most of the mineral residue consisted of opaque oxides (magnesioferrite spinel), quartz and feldspar. These grains are mounted for scanning electron microscope (SEM) analysis, including qualitative chemical analysis, mineralogy, and identification of planar features possibly related to shock metamorphism. Selected grains of magnesioferrite from one sample from Hole 886C were mounted in polished section and analyzed in a CAMEBAX model Cameca electron microprobe. Oxide and silicate standards and ZAF corrections were used. The magnesioferrite grains were analyzed for Mg, Al, Si, Ca, Ti, Cr, Mn, Fe, and Ni. Fe_2O_3 contents of the spinel were calculated assuming stoichiometry by the method of Finger (1972). This calculation occasionally yields slightly negative values for FeO, in which case FeO was recorded as zero. We report results on analyses that totaled between 98% and 102% after correction for Fe^{3+}.

RESULTS

Hole 886C

Concentrations of Co, Cr, and Ir in Hole 886C samples are given in Table 1 and profiles for Ir and Cr at the K/T boundary are illustrated in Figure 2. In our initial survey, several samples had Ir concentrations significantly higher than in adjacent samples. At 55.4 mbsf we obtained a value of 39 ng/g, an extraordinary value that we attribute either to laboratory contamination or to the presence of a large cosmic spherule or Pt-metal nugget from meteoroid ablation (Blanchard et al., 1980; Brownlee et al., 1984; Bonté et al., 1987). Subsequent analyses were unable to replicate this result and we now report a concentration of 0.18 ng/g Ir for this sample. Replicates of a nearby sample at 55.9 mbsf with 1.5 ng/g Ir confirmed this relatively high value. This sample, however, is considered unlikely to contain the K/T boundary, as it is only ~1 m below the Miocene diatomaceous oozes. It has not yet been investigated further in any detail. Another slightly anomalous Ir value of 1.14 ng/g was obtained at 60.80 mbsf, which is ~2× background. This has not been replicated or investigated further. The two highest Ir concentrations measured in our survey of Hole 886C were in two adjacent samples at 65.1 and 65.25 mbsf with Ir at ~3 ng/g each. A small, uncrushed split (~100 mg) of the sample at 65.1 m had been retained and a survey of trace minerals indicated that it contained several quartz grains with planar features, probably from shock deformation. With our subsequent investigation of this interval we have now found 17 consecutive samples from 65.03 to 65.50 mbsf that have Ir with concentrations from 1.5 to 4.0 ng/g. The highest Ir concentrations occur in the interval from 65.12 to 65.25 mbsf, although there is also one high sample at 65.41.

During resampling of this section of core, the sediments were examined with a magnifying glass and no features other than uniform brown clay were observed. However, in the laboratory microscopic examination of fresh surfaces on some cut and broken samples showed several white and yellow spheroids, three of which were hollow, in samples from 65.09 to 65.37 mbsf. These spherules were distinct from abundant manganese micronodules also present. Our trace mineral procedure destroys spherules, but Ingram (this volume) has recovered several spherules in the coarse fraction of a sample from 65.15 to 65.20 mbsf. We prepared a trace mineral residue from a sample at 65.21 mbsf that was atypical of most deep-sea clays, in that it contained numerous millimeter-sized Fe-rich silicate concretions. We think that these were residues of hydrothermal sediments that are abundant at the bottom of this hole. The residue also contained abundant quartz and some magnesioferrite spinel (Table 2). Quartz grains as large as 225 mm with planar features were found and one quartz grain with a maximum diameter of 300 mm was recovered (Pl. 1). These are much larger than shocked quartz previously reported in Pacific K/T boundary sediments in Core LL44-GPC3 (Bohor et al., 1987) or DSDP Site 596 (Zhou et al., 1991). Microprobe analyses of 22 points on 11 grains of spinel from this sample (Table 3) showed that they were magnesioferrite with an average composition approxi-

Table 1. Cr, Co, and Ir concentrations in sediments from Hole 886C.

Core, section, interval (cm)	Depth (mbsf)	Cr (µg/g)	Co (µg/g)	Ir (ng/g)
145-886C-				
1H-1, 75–76	0.75	69	59	0.09
1H-2, 75–76	2.25	65	57	0.11
1H-3, 75–76	3.75	62	51	0.09
1H-4, 75–76	5.25	46	38	0.23
1H-5, 55–56	6.55	67	42	0.08
2H-1, 75–76	7.55	74	55	0.06
2H-2, 75–76	9.05	58	53	0.09
2H-3, 75–76	10.55	64	61	0.14
2H-4, 75–76	12.05	58	56	0.19
2H-5, 75–76	13.55	48	46	0.11
2H-6, 40–41	14.70	27	42	0.04
3H-1, 75–76	17.05	50	52	0.05
3H-2, 75–76	18.55	34	54	0.06
3H-3, 75–76	20.05	40	17	<0.06
3H-4, 75–76	21.55	32	76	<0.06
3H-5, 75–76	23.05	36	114	0.09
3H-6, 56–57	24.36	31	12	<0.05
3H-7, 40–41	25.34	25	7	<0.03
4H-1, 75–76	26.55	20	6	0.06
4H-2, 75–76	28.05	16	18	<0.08
4H-3, 75–76	29.55	10	11	<0.07
4H-4, 75–76	31.05	12	11	<0.12
4H-5, 75–76	32.55	18	8	<0.08
4H-6, 50–51	33.80	14	15	<0.06
4H-7, 35–36	34.65	28	25	<0.04
5H-1, 75–76	36.05	25	20	<0.03
5H-2, 75–76	37.55	15	12	<0.03
5H-3, 75–76	38.80	15	12	<0.04
5H-4, 25–26	39.55	21	18	0.03
6H-1, 75–76	45.55	20	13	0.02
6H-2, 75–76	47.05	23	10	0.02
6H-3, 75–76	48.55	34	14	0.04
6H-4, 25–26	49.55	50	17	0.06
6H-4, 75–76	50.05	49	43	0.12
6H-4, 125–126	50.55	47	67	0.12
6H-5, 25–26	51.05	46	49	0.10
6H-5, 75–76	51.55	46	75	0.15
6H-5, 125–126	52.05	45	37	0.12
6H-6, 25–26	52.55	39	56	0.11
6H-6, 75–76	53.05	61	66	0.17
6H-6, 125–126	53.55	63	70	0.14
6H-7, 25–26	54.05	52	53	0.14
7H-1, 10–11	54.40	62	77	0.15
7H-1, 30–31	54.60	63	82	0.14
7H-1, 50–51	54.80	55	78	0.13
7H-1, 70–71	55.00	57	68	0.15
7H-1, 90–91	55.20	22	23	0.09
7H-1, 110–111	55.40	61	117	0.18
7H-1, 130–131	55.60	46	87	0.17
7H-1, 145–146	55.75	58	117	0.35
7H-2, 10–11	55.90	72	123	1.52
7H-2, 30–31	56.10	65	154	0.37
7H-2, 50–51	56.30	68	152	0.36
7H-2, 70–71	56.50	67	128	0.26
7H-2, 90–91	56.70	59	137	0.21
7H-2, 110–111	56.90	66	138	0.19
7H-2, 130–131	57.10	70	152	0.18
7H-2, 145–146	57.25	68	149	0.47
7H-3, 10–11	57.40	62	136	0.31
7H-3, 30–31	57.60	57	152	0.27
7H-3, 50–51	57.80	51	168	0.34
7H-3, 70–71	58.00	57	195	0.67
7H-3, 90–91	58.20	47	213	0.51
7H-3, 110–111	58.40	45	201	0.62
7H-3, 130–131	58.60	41	270	0.72
7H-3, 145–146	58.75	40	283	0.52
7H-4, 10–11	58.90	43	288	0.72
7H-4, 30–31	59.10	44	225	0.78
7H-4, 50–51	59.30	39	255	0.48
7H-4, 70–71	59.50	48	214	0.46
7H-4, 90–91	59.70	54	195	0.46
7H-4, 110–111	59.90	55	186	0.63
7H-4, 130–131	60.10	56	190	0.64
7H-4, 145–146	60.25	46	184	0.62
7H-5, 10–11	60.40	44	202	0.48
7H-5, 30–31	60.60	51	235	0.67
7H-5, 50–51	60.80	55	187	1.14
7H-5, 70–71	61.00	41	178	0.54
7H-5, 90–91	61.20	36	156	0.40
7H-5, 110–111	61.40	27	154	0.37
7H-5, 130–131	61.60	29	162	0.41
7H-6, 6–7	61.86	10	46	0.12
7H-6, 10–11	61.90	41	123	0.47
7H-6, 30–31	62.10	43	165	0.57
7H-6, 50–51	62.30	46	180	0.66
7H-6, 70–71	62.50	41	178	0.69
7H-6, 90–91	62.70	39	165	0.67
7H-6, 110–111	62.90	42	126	0.57
7H-6, 130–131	63.10	49	134	0.65
7H-6, 145–146	63.25	56	139	0.74
7H-7, 10–11	63.40	60	112	0.50
7H-7, 30–31	63.60	55	97	0.56
7H-7, 45–46	63.75	50	86	0.56
8H-1, 10–11	63.90	43	118	0.79
8H-1, 30–31	64.10	52	146	1.10
8H-1, 50–51	64.30	49	122	0.90
8H-1, 70–71	64.50	52	116	0.83
8H-1, 90–91	64.70	44	107	0.95
8H-1, 110–111	64.90	48	130	1.43
8H-1, 123–124	65.03	58	142	2.20
8H-1, 126–127	65.06	53	133	2.07
8H-1, 129–130	65.09	73	143	2.49
8H-1, 130–131	65.10	55	131	2.96
8H-1, 132–133	65.12	67	154	3.62
8H-1, 135–136	65.15	71	151	3.70
8H-1, 138–139	65.18	58	156	3.61
8H-1, 141–142	65.21	59	134	3.64
8H-1, 144–145	65.24	65	158	4.01
8H-1, 145–146	65.25	53	136	3.11
8H-1, 147–148	65.27	57	183	2.70
8H-2, 2–3	65.32	53	182	1.98
8H-2, 7–8	65.37	54	168	1.98
8H-2, 10–11	65.40	46	157	1.58
8H-2, 11–12	65.41	59	169	3.23
8H-2, 15–16	65.45	57	191	1.81
8H-2, 20–21	65.50	53	194	1.78
8H-2, 30–31	65.60	45	128	1.32
8H-2, 50–51	65.80	45	167	1.29
8H-2, 70–71	66.00	44	164	1.22
8H-2, 90–91	66.20	43	148	1.10
8H-2, 110–111	66.40	40	137	1.15
8H-2, 130–131	66.60	37	125	1.08
8H-2, 145–146	66.75	40	135	1.45
8H-3, 10–11	66.90	38	129	1.18
8H-3, 30–31	67.10	37	129	1.19
8H-3, 50–51	67.30	33	126	1.08
8H-3, 70–71	67.50	30	104	1.12
8H-3, 90–91	67.70	32	95	1.22
8H-3, 110–111	67.90	29	86	1.11
8H-3, 130–131	68.10	27	78	1.14
8H-3, 145–146	68.25	29	77	0.98
8H-4, 10–11	68.40	29	73	1.02
8H-4, 30–31	68.60	29	81	0.97
8H-4, 50–51	68.80	29	84	0.99
8H-4, 70–71	69.00	26	76	0.79
8H-4, 90–91	69.20	28	77	0.82
8H-4, 110–111	69.40	26	78	0.67
8H-4, 130–131	69.60	22	86	0.84
8H-4, 145–146	69.75	23	89	0.94
8H-5, 10–11	69.90	22	81	0.89
8H-5, 30–31	70.10	23	89	0.76
8H-5, 50–51	70.30	26	82	0.76
8H-5, 70–71	70.50	23	82	0.79
8H-5, 90–91	70.70	23	82	0.81
8H-5, 110–111	70.90	28	80	0.79
8H-5, 130–131	71.10	27	82	0.78
8H-6, 10–11	71.40	13	71	0.49
8H-6, 30–31	71.60	13	91	0.40
8H-6, 50–51	71.80	13	73	0.38
8H-6, 70–71	72.00	13	61	0.37
8H-6, 90–91	72.20	13	67	0.34

mated as $(Mg_{.87}Ni_{.09}Fe_{.04})O(Fe_{.79}Al_{.20}Cr_{.01})_2O_3$. More detailed mineralogical analyses are in progress and will be presented elsewhere (J.A. Bostwick, unpubl. data).

Hole 803D

Concentrations of Co, Cr and Ir in Hole 803D sediments are given in Table 4 and profiles for Ir and Cr at the K/T boundary are illustrated in Figure 2. During the initial sampling of this core, F.T. Kyte took an extra sample at 622.43 mbsf because sediments here were distinctly different than those in the rest of the core. From ~622.49 to 622.37 mbsf sediments have a much lighter color than the surrounding dark-brown claystones and at ~622.43 mbsf, thin, millimeter-long patches of white sediment were observed that were suspected to be flattened spheroids. This sample was found to contain 10.8 ng/g Ir. Subsequent analyses of additional samples has confirmed a sharp Ir anomaly with

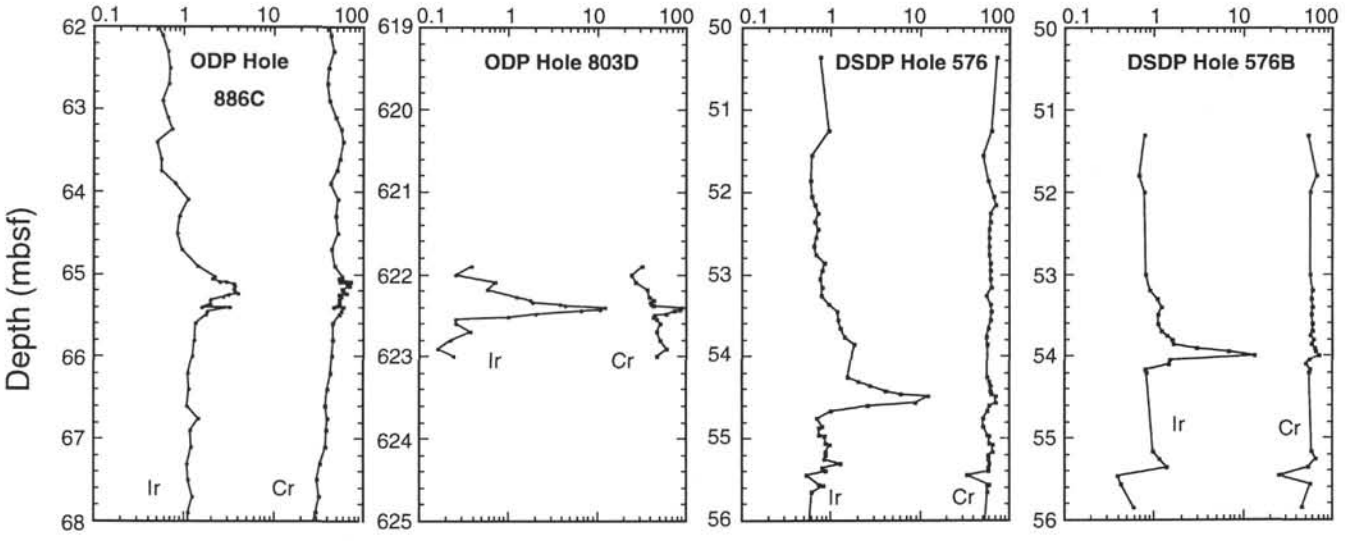

Figure 2. Elemental concentrations of iridium (ng/g) and chromium (μg/g) vs. depth near the K/T boundary in Holes 886C, 803D, 576, and 576B.

Table 2. Quartz in trace mineral separates from K/T boundary sediments.

Core, section interval (cm)	Sample mass (mg)	Quartz grains: Total (>30 μm)	Quartz grains: Shocked (%)	Quartz grains: Largest (μm)	Distance from Chicxulub at 66 Ma (km)
145-886C-8H-1, 141–142	249	301	70	300[a]	6,450
130-803D-63R-1, 63–64	401	112	35	125	11,000
86-576-8-1, 39–41	518	259	65	160	9,100

[a]Largest quartz grain with definite shock lamellae at Hole 886C was 225 μm.

Table 3. Comparison of mean compositions of K/T boundary spinel at Site 886 to that of spinel from DSDP Site 577 and LL44-GPC3 in the North Pacific and from Furlo, Italy.

	Site 886	Site 577	GPC3	Furlo
MgO	18.06	21.02	18.21	9.86
Al_2O_3	11.58	22.07	13.75	3.38
CaO	0.76	0.50	0.62	0.39
TiO_2	0.32	0.32	0.76	0.51
Cr_2O_3	1.20	0.20	0.34	0.66
MnO	0.39	0.58	1.13	1.15
FeO	3.06	0.55	2.78	9.90
Fe_2O_3	63.36	53.42	60.62	68.44
NiO	1.62	1.41	1.40	5.48
SiO_2	0.08	0.12	0.34	0.02
Total	100.55	100.19	99.95	99.79

Note: Data for DSDP Site 577, Core LL44-GPC3, and Furlo are from Kyte and Smit (1986).

a peak of 12.1 ng/g Ir at 622.41 mbsf and Ir concentrations above background (>1 ng/g) over at least 24 cm from 622.28 to 622.52 mbsf. A trace mineral separate was been prepared for a sample from 622.43 mbsf. Abundant quartz grains with planar features and Ni-rich magnesioferrite grains were observed (Table 2, Pl. 1).

Holes 576 and 576B

Iridium anomalies have been found in both of these holes (Table 5, Fig. 2). Interestingly, the anomalies are at significantly different depths relative to prominent calcareous turbidites found in the uppermost Cretaceous at this site (Heath, Burckle, et al., 1985). As a result, the K/T anomalies in these two holes do not have identical assigned depths (based on composite sections of Heath et al., 1985). Also, the Ir peak is considerably thicker in Hole 576 than in 576B, although both holes have similar maximum Ir concentrations (12 to 13 ng/g). This latter discrepancy may be exacerbated by the fact that the upper tail of the Ir anomaly in Hole 576 is intersected by a core break. In their composite section, Heath et al. (1985) placed a gap between cores 86-576-7 and 86-576-8. Our data indicate that in fact, there may be an overlap between these cores. Analyses of trace minerals from 12 samples across the Ir anomaly in Hole 576B yielded virtually no mineral grains >30 μm except in three samples exactly in the Ir anomaly (J.A. Bostwick, unpubl. data). In these samples we found abundant quartz grains, several with planar features, and magnesioferrite spinel (Table 2, Pl. 1).

DISCUSSION

We are convinced that we have accurately identified the K/T boundary at each of these three sites. At Site 576 the Ir anomaly is within the ichthyolith-defined region that should contain the K/T boundary (Doyle and Riedel, 1985). At Site 803, the anomaly is just ~12 cm below the depth defined by poorly preserved nannofossils. At Site 886, we have no biostratigraphic constraints other than late Miocene diatomaceous oozes overlying 18 m of pelagic clay. However, basement basalts have been dated at 80 Ma (Keller et al., 1993) so Cretaceous-age sediments should be present at this site. Additionally, the Ir anomaly in Hole 886C has all the chemical and mineralogical properties characteristic of the K/T boundary. These properties, which apply to all three sites are (1) a large, reproducible Ir anomaly with a net Ir fluence comparable to other K/T localities around the world, (2) a significant enrichment of Cr within the Ir anomaly, (3) large quartz grains, many of which have planar features, and (4) Ni-rich magnesioferrite spinel. Additionally, spheroidal material has been observed at Sites 576 and 886.

Our best estimates of the net Ir fluences in these anomalies are 52, 140, 130, and 90 ng Ir cm^{-2} in Holes 886C, 803D, 576 and 576B,

Table 4. Cr, Co, and Ir concentrations in sediments near the K/T boundary in Hole 803D.

Core, section, interval (cm)	Depth (mbsf)	Cr (μg/g)	Co (μg/g)	Ir (ng/g)
130-803D-				
68R-1, 10–11	621.90	32	46	0.38
68R-1, 20–21	622.00	24	47	0.25
68R-1, 29–30	622.09	27	51	0.71
68R-1, 39–40	622.19	36	36	0.57
68R-1, 48–49	622.28	38	30	1.24
68R-1, 51–52	622.31	43	56	1.78
68R-1, 54–55	622.34	39	68	1.86
68R-1, 57–58	622.37	41	22	3.77
68R-1, 58–59	622.38	43	28	4.33
68R-1, 61–62	622.41	87	28	12.1
68R-1, 63–64	622.43	86	26	10.8
68R-1, 64–65	622.44	74	27	6.45
68R-1, 68–69	622.48	60	31	2.02
68R-1, 70–71	622.50	44	56	NA
68R-1, 72–73	622.52	43	61	1.00
68R-1, 75–76	622.55	47	86	0.25
68R-1, 80–81	622.60	51	71	0.25
68R-1, 90–91	622.70	47	109	0.37
68R-1, 100–101	622.80	51	87	0.22
68R-1, 110–111	622.90	59	54	0.16
68R-1, 120–121	623.00	47	61	0.24

Note: NA = not analyzed.

respectively. By comparison, typical Ir fluences in K/T boundaries around the globe have been estimated to average in the range of ~60 to 100 ng Ir cm^{-2} (Kyte et al., 1985; Strong et al., 1987), and those at other sites in the Pacific range from 61 (DSDP Site 577; Michel et al., 1985) to 320 ng Ir cm^{-2} (DSDP Site 596; Zhou et al., 1991). The anomalies at these three new sites are all somewhat typical of the global marine K/T boundary. The Ir anomaly in Hole 803D appears much sharper than at the other two sites (Fig. 2), but this is an artifact of compaction. On the basis of sediment dry densities (Kroenke, Berger, Janecek, et al., 1991; Rea, Basov, Janecek, Palmer-Julson, et al., 1993), we find that Hole 803D (1.4 g/cm^3) has been compacted by a factor of 2.6 relative to Hole 886C (0.54 g/cm^3). We assume that the breadth of the Ir anomalies at all three sites is largely caused by reworking of an initially thin deposit, probably by bioturbation. Reworking at Hole 886C is indicated by the large vertical distribution of spheroidal material. However, we cannot rule other possible factors such as chemical diffusion of Ir or distortion of sediment cores during hydraulic piston coring.

The Cr enrichment is also significant. Of all the elements that can be measured by INAA in transition metal-rich pelagic clays, only Cr tends to show a small enrichment along with Ir (Zhou et al., 1991). This is likely because the Cr/Ir ratio in CI chondrites is ~6000 (Wasson, 1985). Based on a CI chondrite source for the Ir and no chemical fractionation of Cr relative to Ir, we would anticipate Cr enrichments above background that range from ~30 μg/g (Hole 886C) to 70 μg/g (576). Observed Cr enrichments are close to such model values in Holes 886C (~20 μg/g) and 803D (~50 μg/g). At Site 576, Cr enrichment is less than predicted by this model (~15–20 μg/g), but still significantly above backgrounds.

We need to note that SEM identification of planar features is not absolutely conclusive evidence of shock deformation. Ideally, individual quartz grains should be analyzed by optical microscopy using spindle- or universal-stage methods to measure angles of planar features relative to the crystallographic axes (von Engelhardt and Bertsch, 1969; Stöffler, 1972); such analyses are planned. Nonetheless, many of the grains we have examined by SEM exhibit several features diagnostic of shock, including multiple sets of very straight planar features that extend entirely across the grain. (French and Short, 1968). Also, these quartz grains are enormous (up to 300 μm) compared to typical eolian quartz grains in Pacific pelagic clays (mean sizes of 8–9 μm; Rea et al., 1985; Janecek and Rea, 1983).

The magnesioferrite compositions are highly diagnostic of K/T boundary sediments. Ni-rich magnesioferrites are known to occur

Table 5. Cr, Co, and Ir concentrations in sediments near the K/T boundary in DSDP Holes 576 and 576B.

Core, section, interval (cm)	Depth (mbsf)	Cr (μg/g)	Co (μg/g)	Ir (ng/g)
86-576-				
7-4, 145–147	50.36	72	185	0.75
7-5, 85–87	51.26	63	207	0.93
7-5, 115–117	51.56	51	216	0.61
7-5, 145–147	51.86	58	201	0.59
7-6, 15–17	52.06	66	188	0.61
7-6, 25–27	52.16	70	197	0.66
7-6, 35–37	52.26	61	199	0.71
7-6, 45–47	52.36	61	200	0.65
7-6, 55–57	52.46	60	196	0.72
7-6, 65–67	52.56	60	188	0.68
7-6, 75–77	52.66	59	183	0.64
7-6, 85–87	52.76	59	191	0.68
7-6, 95–97	52.86	62	192	0.83
7-6, 105–107	52.96	62	192	0.80
7-6, 115–117	53.06	61	176	0.76
7-6, 125–127	53.16	63	171	0.80
7-6, 135–137	53.26	55	157	0.78
7-6, 145–147	53.36	61	167	0.94
7-7, 5–7	53.46	63	173	1.15
7-7, 15–17	53.56	61	172	1.19
7-7, 25–27	53.66	58	169	1.28
7-7, 35–37	53.76	55	169	1.40
7-7, 45–47	53.86	57	181	1.81
8-1, 7–8	53.18	59	174	0.79
8-1, 14–16	54.25	57	193	1.54
8-1, 20–22	54.30	59	201	2.00
8-1, 25–27	54.36	61	186	2.74
8-1, 32–34	54.42	62	180	4.09
8-1, 35–37	54.46	63	178	5.94
8-1, 39–41	54.49	70	209	12.31
8-1, 45–47	54.56	71	222	8.75
8-1, 50–52	54.60	60	223	2.57
8-1, 56–58	54.66	56	232	0.98
8-1, 65–67	54.76	51	229	0.69
8-1, 75–77	54.86	51	243	0.80
8-1, 77–79	54.87	52	242	0.73
8-1, 85–87	54.96	57	230	0.74
8-1, 87–89	54.97	60	257	0.84
8-1, 95–97	55.06	60	273	0.86
8-1, 98–100	55.08	64	304	0.97
8-1, 105–107	55.16	64	255	0.86
8-1, 110–112	55.20	58	225	0.87
8-1, 115–117	55.26	58	200	0.85
8-1, 120–122	55.30	60	317	1.27
8-1, 125–127	55.36	58	278	0.79
8-1, 130–132	55.40	58	270	0.87
8-1, 135–136	55.45	34	143	0.53
8-1, 145–147	55.56	59	264	0.74
8-1, 147–148	55.57	57	287	0.82
8-2, 4–6	55.65	56	209	0.61
8-2, 66–68	56.27	52	209	0.56
8-2, 77–79	56.38	54	196	0.89
8-2, 105–107	56.66	49	196	0.69
8-2, 135–137	56.96	54	172	0.57
8-3, 146–148	58.57	53	126	0.45
86-576B-				
6-3, 1–3	51.31	53	202	0.77
6-3, 50–51	51.80	66	203	0.67
6-3, 70–72	52.00	57	165	0.77
6-3, 91–92	53.01	56	169	0.79
6-3, 110–111	53.20	59	166	0.89
6-3, 120–121	53.30	58	174	1.08
6-3, 130–132	53.40	60	182	1.20
6-3, 140–141	53.50	58	177	1.10
6-4, 1–3	53.61	60	189	1.12
6-4, 10–11	53.70	59	188	1.20
6-4, 15–15	53.75	56	182	1.37
6-4, 20–21	53.80	61	195	1.57
6-4, 25–27	53.85	58	196	1.61
6-4, 30–31	53.90	63	197	2.94
6-4, 35–37	53.95	65	192	6.79
6-4, 40–42	54.00	70	216	13.43
6-4, 45–47	54.05	55	245	1.50
6-4, 50–52	54.10	50	247	1.44
6-4, 56–57	54.16	56	262	0.79
6-4, 60–61	54.20	55	270	0.81
6-4, 70–71	55.16	58	288	0.97
6-4, 80–81	55.26	65	226	1.15
6-4, 90–91	55.36	54	284	1.38
6-4, 100–101	55.46	25	99	0.39
6-4, 110–112	55.56	57	200	0.42
6-4, 138–139	55.84	45	190	0.59

Note: Depths are based on composite section of Heath et al. (1985).

only in K/T boundary sediments (commonly in spherules; e.g., Smit and Kyte, 1984), in spherules produced by an oceanic asteroid impact in the late Pliocene (Margolis et al., 1991), and in chondritic cosmic spherules and meteorite fusions crusts (Robin et al., 1992). The magnesioferrites from the K/T boundary are distinct from those found in cosmic spherules which have considerably lower concentrations of MgO and Al_2O_3 and lower Fe_2O_3/FeO ratios (Robin et al., 1992). However, the Site 886 spinel (Table 3) are very similar to, and hardly distinguishable from, compositions reported for spinel in North Pacific K/T boundaries at DSDP Site 577 and LL44-GPC3 (Kyte and Smit, 1986).

Finally, we would like to point out that placing the K/T boundary at ~65.2 mbsf in Hole 886C is roughly consistent with Co accumulation rates. Zhou and Kyte (1992) and Kyte et al. (1993) have used Co accumulation rates in an attempt to constrain bulk sediment accumulation rates in DSDP Hole 596 and LL44-GPC3, respectively. They noted that among the 35 to 39 elements they measured, Co could be demonstrated to accumulate at the most constant rate. Although this technique is bound to be imperfect, their rationale was that accumulation rates in pelagic clays are so poorly constrained by any other method that fitting clay sections with a model accumulation rate curve was superior to using a single value based on linear sedimentation rates.

We lack the data to duplicate the sediment component models that Zhou and Kyte (1992) and Kyte et al. (1993) used to derive estimates of hydrogenous Co accumulation, so for Hole 886C we can only address this problem qualitatively using bulk Co accumulation. Estimates of Cenozoic hydrogenous Co accumulation in DSDP Hole 596 and LL44-GPC3 were 1.99 and 2.3 mg cm^{-2} Ma^{-1}, respectively. Our estimate of the total Co accumulation in the pelagic clay Unit III of Hole 886C (54.3 to 72.4 mbsf; Rea, Basov, Janecek, Palmer-Julson, et al., 1993) is 130 mg. Of this amount, 96 mg is from above the K/T boundary and 34 is from the K/T boundary to basement. Given a late Miocene age of 10 Ma for 54.3 mbsf (Rea, Basov, Janecek, Palmer-Julson, et al., 1993) and 80 Ma for basaltic basement, the average Co accumulation rate in Unit III is 1.86 mg cm^{-2} Ma^{-1}. Given the uncertainties in sediment dry densities, this value is undistinguishable from the 1.99 mg cm^{-2} Ma^{-1} used in DSDP Hole 596. If we were to extrapolate from 54.3 mbsf using a Co accumulation rate of 1.86 mg cm^{-2} Ma^{-1}, we would have predicted that the K/T boundary is at 66.2 mbsf, only 1 m below the actual boundary. We note that Dickens et al. (this volume) have reported that there is evidence for a gap between Cores 145-886C-7H and -8H, which they have estimated could be ~0.75 m, although there are no firm data to exclude an even larger gap. Any gap will increase the actual Co accumulation rate over our estimate and would cause our estimate of the K/T boundary location based on Co accumulation to be closer to the measured Ir anomaly.

CONCLUSIONS

Geochemical and mineralogical analyses have been used to identify the K/T boundary at three Pacific drill sites; ODP Sites 886 and 803 and DSDP Site 576. At each site the K/T boundary is characterized by an Ir anomaly, coincident with a small enrichment of Cr, abundant quartz grains with planar features typical of shock metamorphism, and Ni-rich magnesioferrite spinel.

ACKNOWLEDGMENTS

We thank B.F. Bohor and C.J. Orth for their reviews and B.L. Ingram and G.R. Dickens for allowing us to view their results on Hole 886C. Sediment cores are curated with support by the NSF. This research was supported by NSF grant EAR-91-18701.

REFERENCES*

Alvarez, L.W., Alvarez, W., Asaro, F., and Michel, H.V., 1980. Extraterrestrial cause for the Cretaceous-Tertiary extinction. *Science,* 208:1095–1108.

Blanchard, M.B., Brownlee, D.E., Bunch, T.E., Hodge, P.W., and Kyte, F.T., 1980. Meteoroid ablation spheres from deep-sea sediments. *Earth Planet. Sci. Lett.,* 97:162–176.

Bohor, B.F., Foord, E.E., and Ganapathy, R., 1986. Magnesioferrite from the Cretaceous-Tertiary boundary, Caravaca, Spain. *Earth Planet. Sci. Lett.,* 81:57–66.

Bohor, B.F., Modreski, P.J., and Foord, E.E., 1987. Shocked quartz in the Cretaceous/Tertiary boundary clay: evidence for a global distribution. *Science,* 236:705–709.

Bonté, P., Jéhanno, C., Maurette, M., Brownlee, D.E., 1987. Platinum metals and microstructure in magnetic deep sea cosmic spherules. *In* Ryder, G., and Schubert, G. (Eds.), *Proc. Lunar Planet. Sci. Conf. 17th, Pt. 2.* J. Geophys. Res., 92:E641–E648.

Brownlee, D.E., Bates, B.A., and Wheelock, M.M., 1984. Extraterrestrial platinum group nuggets in deep sea sediments. *Nature,* 309:693–695.

Doyle, P.S., and Riedel, W.R., 1985. Ichthyolith biostratigraphy of western North Pacific pelagic clays, Deep Sea Drilling Project Leg 86. *In* Heath, G.R., Burckle, L.H., et al., *Init. Repts. DSDP,* 86: Washington (U.S. Govt. Printing Office), 349–366.

Finger, L.W., 1972. The uncertainty in the calculated ferric iron content of a microprobe analysis. *Year Book—Carnegie Inst. Washington,* 71:600–603.

French, B.M., and Short, N.M., 1968. *Shock Metamorphism of Natural Materials:* Baltimore (Mono Book Corp.).

Ganapathy, R., 1980. A major meteorite impact on the Earth 65 million years ago: evidence from the Cretaceous-Tertiary boundary clay. *Science,* 209:921–923.

Heath, G.R., Burckle, L.H., et al., 1985. *Init. Repts. DSDP,* 86: Washington (U.S. Govt. Printing Office).

Heath, G.R., Kovar, R.B., Lopez, C., and Campi, G.L., 1985. Elemental composition of Cenozoic pelagic clays from Deep Sea Drilling Project Sites 576 and 578, western North Pacific. *In* Heath, G.R., Burckle, L.H., et al., *Init. Repts. DSDP,* 86: Washington (U.S. Govt. Printing Office), 605–646.

Hildebrand, A.R., Penfield, G.T., Kring, D.A., Pilkington, M., Camargo, A.Z., Jacobsen, S.B., and Boynton, W.V., 1991. Chicxulub crater: a possible Cretaceous/Tertiary boundary impact crater on the Yucatán Peninsula, Mexico. *Geology,* 19:867–871.

Izett, G.A., 1990. The Cretaceous/Tertiary boundary interval, Raton Basin, Colorado and New Mexico, and its content of shock-metamorphosed minerals: evidence relevant to the K/T boundary impact-extinction theory. *Spec. Pap.—Geol. Soc. Am.,* 249.

Janecek, T.R., and Rea, D.K., 1983. Eolian deposition in the northeast Pacific Ocean: Cenozoic history of atmospheric circulation. *Geol. Soc. Am. Bull.,* 94:730–738.

Keller, R.A., and the Leg 145 Shipboard Scientific Party, 1993. Age and geochemistry of basaltic basement recovered during ODP Leg 145 (North Pacific Transect). *Eos,* 74:355. (Abstract)

Kroenke, L.W., Berger, W.H., Janecek, T.R., et al., 1991. *Proc. ODP, Init. Repts.,*130: College Station, TX (Ocean Drilling Program).

Kyte, F.T., Leinen, M., Heath, G.R., and Zhou, L., 1993. Cenozoic sedimentation history of the central North Pacific: inferences from the elemental geochemistry of Core LL44-GPC3. *Geochim. Cosmochim. Acta,* 57:1719–1740.

Kyte, F.T., and Smit, J., 1986. Regional variations in spinel compositions: an important key to the Cretaceous/Tertiary event. *Geology,* 14:485–487.

Kyte, F.T., Smit, J., and Wasson, J.T., 1985. Siderophile interelement variations in the Cretaceous/Tertiary boundary sediments from Caravaca, Spain. *Earth Planet. Sci. Lett.,* 73:183–195.

Kyte, F.T., and Wasson, J.T., 1986. Accretion rate of extraterrestrial matter: iridium deposited 33 to 67 million years ago. *Science,* 232:1225–1229.

Kyte, F.T., Zhou, Z., and Wasson, J.T., 1980. Siderophile-enriched sediments from the Cretaceous/Tertiary boundary. *Nature,* 288:651–656.

* Abbreviations for names of organizations and publications in ODP reference lists follow the style given in *Chemical Abstracts Service Source Index* (published by American Chemical Society).

Margolis, S., Claeys, Ph., and Kyte, F.T., 1991. Microtektites, microkrystites and spinels from a late Pliocene asteroid impact in the Southern Ocean. *Science,* 251:1594–1597.

Michel, H.V., Asaro, F., Alvarez, W., and Alvarez, L.W., 1985. Elemental profile of iridium and other elements near the Cretaceous/Tertiary boundary in Hole 577B. *In* Heath, G.R., Burckle, L.H., et al., *Init. Repts. DSDP,* 86: Washington (U.S. Govt. Printing Office), 533–538.

Montanari, A., Hay, R.L., Alvarez, W., Asaro, F., Michel, H.V., Alvarez, L.W., and Smit, J., 1983. Spheroids at the Cretaceous/Tertiary boundary are altered impact droplets of basaltic composition. *Geology,* 11:668–671.

Rea, D.K., Basov, I.A., Janecek, T.R., Palmer-Julson, A., et al., 1993. *Proc. ODP, Init. Repts.,* 145: College Station, TX (Ocean Drilling Program).

Rea, D.K., Leinen, M., and Janecek, T.R., 1985. A geological approach to the long-term history of atmospheric circulation. *Science,* 227:721–725.

Robin, E., Bonté, Ph., Froget, L., Jéhanno, C., and Rocchia, R., 1992. Formation of spinels in cosmic objects during atmospheric entry: a clue to the Cretaceous/Tertiary boundary event. *Earth Planet. Sci. Lett.,* 108:181–190.

Sepkoski, J., 1982. Mass extinctions in the Phanerozoic oceans: a review. *Spec. Pap.—Geol. Soc. Am.,* 190:283–289.

Sharpton, V.L., Dalrymple, G.R., Marin, L.E., Ryder, G., Schuraytz, B.C., and Urrutia-Fucugauchi, J., 1992. New links between the Chicxulub impact structure and the Cretaceous/Tertiary boundary. *Nature,* 359:819–821.

Smit, J., and Hertogen, J., 1980. An extraterrestrial event at the Cretaceous/Tertiary boundary. *Nature,* 285:198–200.

Smit, J., and Klaver, G., 1981. Sanidine spherules at the Cretaceous/Tertiary boundary indicate a large impact event. *Nature,* 292:47–49.

Smit, J., and Kyte, F.T., 1984. Siderophile-rich magnetic spheroids from the Cretaceous/Tertiary boundary in Umbria, Italy. *Nature,* 310:403–405.

Smit, J., Montanari, A., Swinburne, N.H.M., Alvarez, W., Hildebrand, A.R., Margolis, S.V., Claeys, Ph., Lowrie, W., and Asaro, F., 1992. Tektite-bearing, deep-water clastic unit at the Cretaceous/Tertiary boundary in northeastern Mexico. *Geology,* 20:99–103

Stöffler, D., 1972. Deformation and transformation of rock-forming minerals by natural and experimental processes: E. Behavior of minerals under shock compression. *Fortschr. Mineral.,* 49:50–113.

Strong, C.P., Brooks, R.R., Wilson, S.M., Reeves, R.D., Orth, C.J., Mao, X., Quintana, L.R., and Anders, E., 1987. A new Cretaceous/Tertiary boundary site at Flaxbourne River, New Zealand: biostratigraphy and geochemistry. *Geochim. Cosmochim. Acta,* 51:2769–2777.

Thiede, J., Vallier, T.L., et al., 1981. *Init. Repts. DSDP,* 62: Washington (U.S. Govt. Printing Office).

von Engelhardt, W., and Bertsch, W., 1969. Shock induced planar deformation structures in quartz from the Ries Crater, Germany. *Contrib. Mineral. Petrol.,* 20:203–234.

Wasson, J.T., 1985. *Meteorites: Their Record of Early Solar-System History:* New York (Freeman).

Zhou, L., and Kyte, F.T., 1992. Sedimentation history of the south Pacific pelagic clay province over the last 85 million years inferred from the geochemistry of Deep Sea Drilling Project Hole 596. *Paleoceanography,* 7:441–465.

Zhou, L., Kyte, F.T., and Bohor, B.F., 1991. The Cretaceous/Tertiary boundary of DSDP Site 596, South Pacific. *Geology,* 19:694–697.

Date of initial receipt: 4 April 1994
Date of acceptance: 19 September 1994
Ms 145SR-132

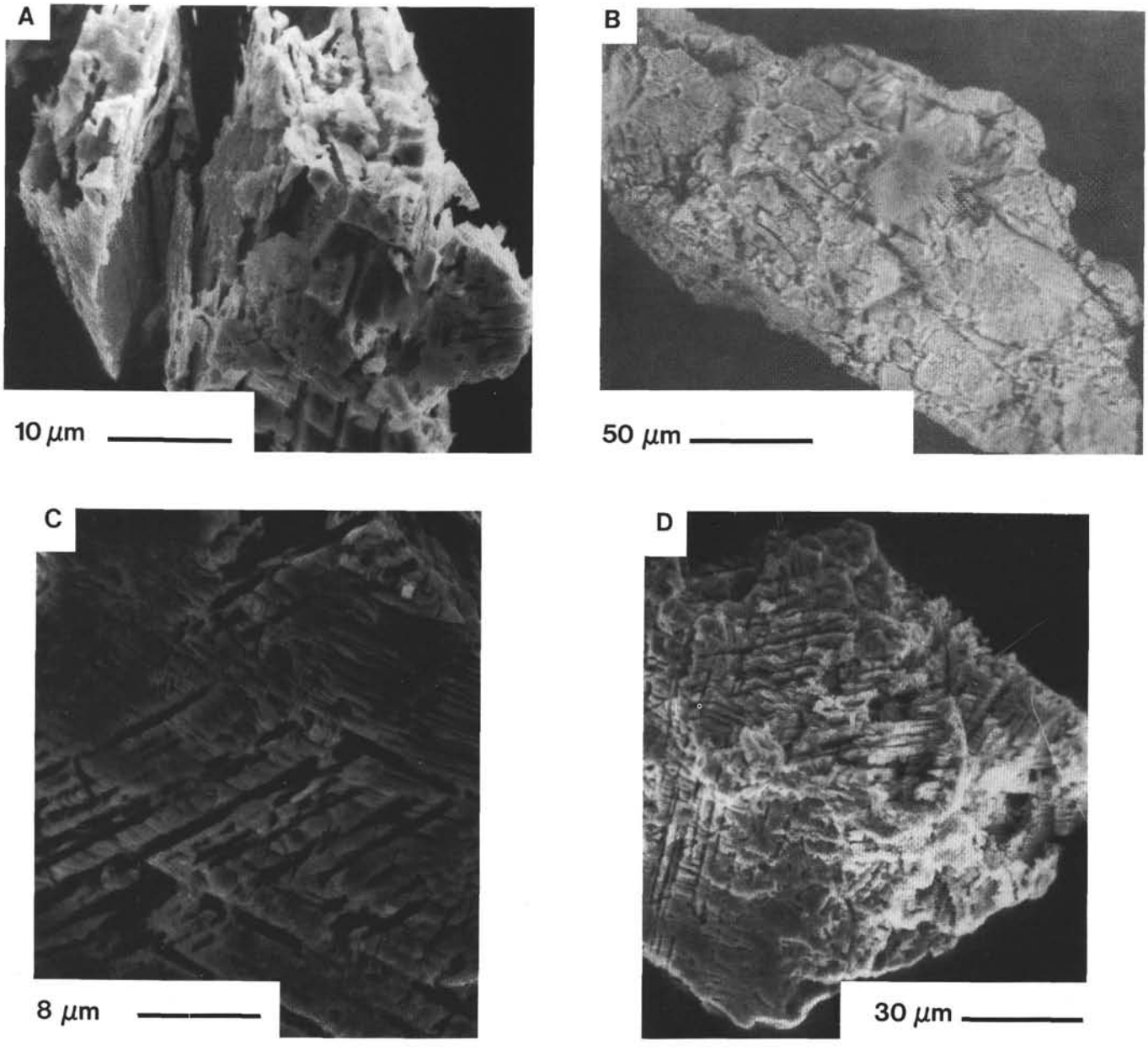

Plate 1. SEM images of quartz grains from the K/T boundary at three Pacific sites. **A.** A very fragile, fragmented grain from Sample 145-886C-8H-1, 141–142 cm, showing at least two sets of planar deformation features. **B.** An extraordinarily large grain (300 μm, maximum diameter) from Hole 886C. Although faint linear features are present, no clear evidence of planar deformation features exist. **C.** A high magnification of the surface of a grain from Sample 130-803D-63R-1, 63–64 cm, displaying four clear sets of planar deformation features. **D.** A brittle-looking grain from Sample 86-576-8-1, 39–41 cm, displaying four sets of planar deformation features.